Nuclear spin determination of 100mY by collinear laser spectroscopy of optically pumped ions

K Baczynska, J Billowes, P Campbell, F C Charlwood, B Cheal, T Eronen, D H Forest, A Jokinen, T Kessler, I D Moore, et al.

Nuclear spin determination of ^{100m}Y by collinear laser spectroscopy of optically pumped ions.

K Baczynska[1], J Billowes[2], P Campbell[2], F C Charlwood[2], B Cheal[2], T Eronen[3], D H Forest[1], A Jokinen[3], T Kessler[3], I D Moore[3], M Rüffer[1], G Tungate[1] and J Äystö[3]

[1] School of Physics and Astronomy, University of Birmingham, Birmingham B15 2TT, United Kingdom

[2] Schuster Laboratory, University of Manchester, Manchester M13 9PL, United Kingdom

[3] Department of Physics, University of Jyväskylä, PB 35 (YFL) FIN-40351 Jyväskylä, Finland

E-mail: k.a.baczynska@gmail.com

Abstract. The nuclear spin of the $\tau_{1/2} = 0.94$ s isomer in ^{100}Y has been determined by collinear laser spectroscopy of optically pumped yttrium fission fragments at the IGISOL facility, JYFL. The isotopes ^{96,98,99,100}Y were produced by proton induced fission of natural uranium, and studied on the 4d5s $^3D_2$ (1045 cm^{-1}) $\rightarrow$ 4d5p $^3P_1$ (32124 cm^{-1}) transition at 321.67 nm. Enhancement of the population of the metastable $^3D_2$ level was achieved by optically pumping the ground state population via the 5s^2 $^1S_0 \rightarrow$ 4d5p $^1P_1$ transition at 363.31 nm while the ions were stored in a linear Paul trap. This data, when combined with previous spectroscopic results, gives sufficient information for the nuclear spin of ^{100m}Y to be determined unambiguously as $I = 4$. This spin assignment reveals that ^{100m}Y has an unexpectedly large dynamic contribution to its quadrupole deformation.

PACS numbers: 21.10.Ft, 21.10.Hw, 21.10.Ky, 42.62.Fi

Submitted to: *J. Phys. G: Nucl. Part. Phys.*

1. Region of the sudden onset of deformation around $Z = 40$

Nuclear structure close to the $Z = 40$ subshell has been the subject of extensive interest for many years. Studies of this region have included recent precise mass determinations [1, 2], γ-spectroscopy [3, 4] and optical measurements. The optically measured Kr [5], Rb [6], Sr [7, 8, 9], Y [10], Zr [11, 12], Nb [13] and Mo [14] isotope chains provide considerable experimental information about ground and isomeric state properties. In the cases of Rb and Sr, the optical measurements revealed two regions of strong ground state deformation, with static quadrupole deformation parameters $\langle\beta_2\rangle \approx 0.4$, for $N \approx 38$ and $N \approx 60$. The Zr, Y and Nb isotopes were subsequently measured using collinear laser spectroscopy and all three isotope chains also show a sharp onset of strong deformation at $N = 60$. Figure 1 illustrates the change in mean–square charge radius as a function of the neutron number and shows the similarities of these isotope chains. The Kr isotope chain measurements show that the evolution of the mean–square charge radius is similar to that in higher Z chains, except at the neutron number $N = 60$. The lack of a sudden onset of deformation at $N = 60$ sets the lower limit in Z for this phenomenon. The corresponding upper limit in Z for this shape change has recently been determined from measurements of the Mo isotope chain. Figure 1 shows that the charge radius in this system increases smoothly from the $N = 50$ shell closure across $N = 60$ with no sudden increase.

The sudden shape change from soft, weakly oblate to more rigid, strongly prolate shapes observed for the isotopes with $42 > Z > 36$ has also been studied theoretically. Shell model calculations attribute the onset of deformation to the isoscalar component of the n–p interaction between nucleons in the spin–orbit partner orbitals $(1g_{9/2})_\pi$ and $(1g_{7/2})_\nu$ [15]. However, mean–field models explain the deformation in terms of the occupation of low K components of the $(1h_{11/2})_\nu$ orbital [16]. Recent calculations using the projected shell model suggest that both of these mechanisms play a rôle in the sudden onset of strong deformation at $N = 60$ [17].

1.1. Yttrium study

The main interest of the odd–Z yttrium chain ($Z = 39$) was based on the investigation of the nuclear shapes and deformations along the isotope chains in the region of $Z = 40$. The yttrium study was especially important for the region between the neutron shell closure and onset of strong deformation in order to address the lack of information on quadrupole moments and deformations for strontium [8] and zirconium isotopes [11].

Isotope shift and hyperfine structure measurements provide complementary information about the nuclear deformation. There are two main contributions to the mean–square charge radius $\langle r^2\rangle$: the nuclear size, and mean–square deformation. Any variation from a spherical shape contributes to the mean–square charge radius and to the lowest order in deformation, $\langle r^2\rangle$ is given by:

$$\langle r^2\rangle = \langle r^2\rangle_s \left(1 + \frac{5}{4\pi}\left\langle\beta_2^2\right\rangle\right) \tag{1}$$

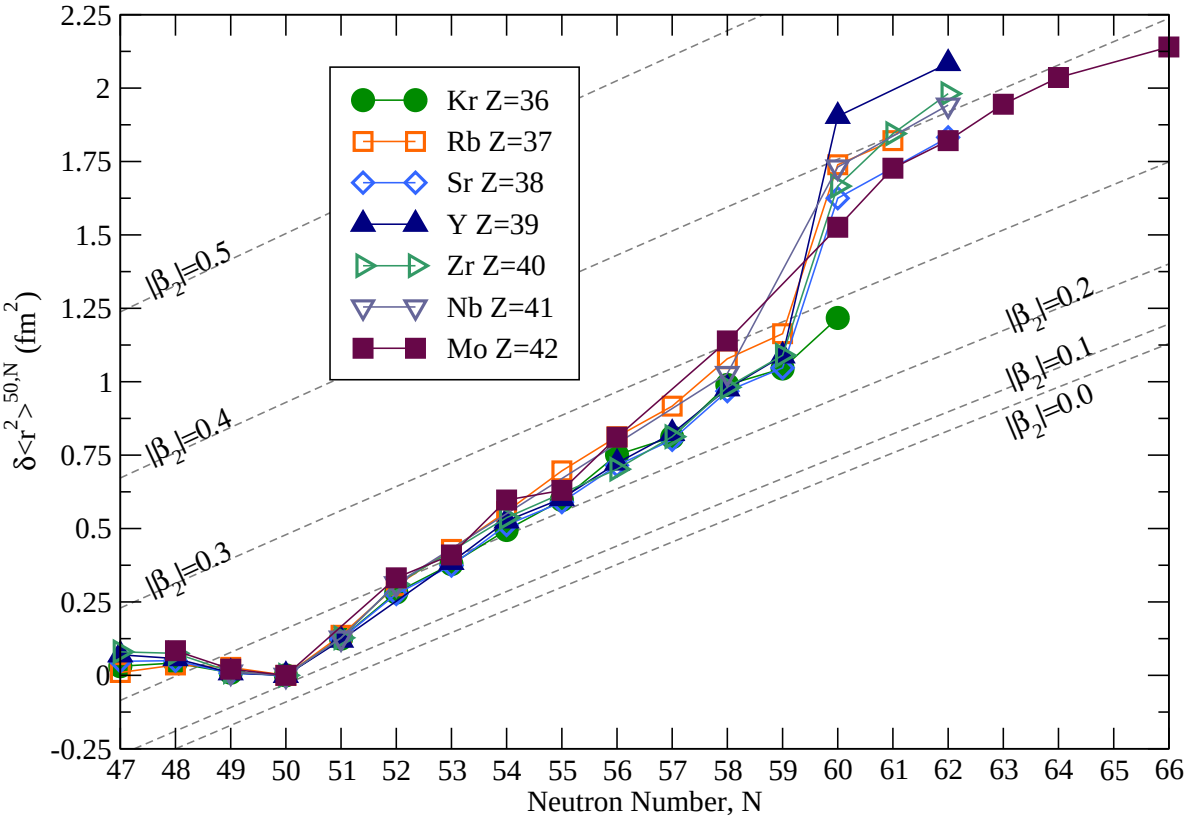

Figure 1. Changes in mean–square charge radii for Kr, Rb, Sr, Y, Zr, Nb and Mo isotope chains. The dashed lines show the predictions of the finite–range droplet model [18] for yttrium.

where $\langle r^2 \rangle_s$ is the mean–square charge radius of an equivalent volume spherical nucleus, which can be calculated from the liquid drop model, or more reliably from the finite–range droplet model of Myers and Schmidt [18], and $\langle \beta_2^2 \rangle$ is the mean–square quadrupole deformation parameter which includes both static and dynamic contributions:

$$\left\langle \beta_2^2 \right\rangle = \langle \beta_2 \rangle^2 + \left(\left\langle \beta_2^2 \right\rangle - \langle \beta_2 \rangle^2 \right) = \beta_{static}^2 + \beta_{dynamic}^2 \tag{2}$$

The deformation, $\langle \beta_2 \rangle$, may be extracted from the hyperfine structure via the electric quadrupole interaction term, which provides the spectroscopic electric quadrupole moment, Q_s. This can be related to $\langle \beta_2 \rangle$ via the projection from the intrinsic frame [19]:

$$Q_s = Q_0 \left[\frac{I\,(2I-1)}{(I+1)\,(2I+3)} \right] \tag{3}$$

and the relation

$$Q_0 \approx \frac{5Z\langle r^2 \rangle_s}{\sqrt{5\pi}} \langle \beta_2 \rangle \,(1 + 0.36\,\langle \beta_2 \rangle) \tag{4}$$

It is evident from (3) that Q_s can only be measured for isotopes with nuclear spins $I \geq 1$. The lack of quadrupole moment information for the Sr and Zr isotope chains is due to many of their odd–A isotopes having ground state spins of $I = 1/2$.

In order to define the nuclear behaviour in this region the isotopes $^{86-90,92-102}$Y have been measured using collinear laser spectroscopy at the IGISOL facility at the University of Jyväskylä, Finland. The strong transition from the Y^+ ground state, $5s^2\ ^1S_0 \rightarrow 4d5p\ ^1P_1$ at 363.31 nm, was used in two experiments reported in reference [10]. The isotope shift and hyperfine structure analysis of these data provided the magnetic dipole, μ, and spectroscopic electric quadrupole, Q_s, moments and changes in mean–square charge radii, $\delta\langle r^2\rangle$. These showed that below the $N = 50$ shell closure, the isomers at least are oblate with significant dynamic deformation, which is demonstrated by the large difference between the measured $\langle r^2\rangle$ and that calculated from (1) using only the contribution from the static deformation, as shown in figure 2.

As the neutron number increases from $N = 50$ the nuclear deformation exhibits an increasingly oblate and increasingly soft nature [10]. At $N = 60$ there is a sudden change to more rigid, strongly deformed prolate shapes.

Yttrium isotopes seem to follow the Rb, Sr and Zr trends. The large shift observed at $N = 59$ between the ^{98}Y ground and isomeric states is a consequence of the nuclear shape changing from oblate to strongly prolate.

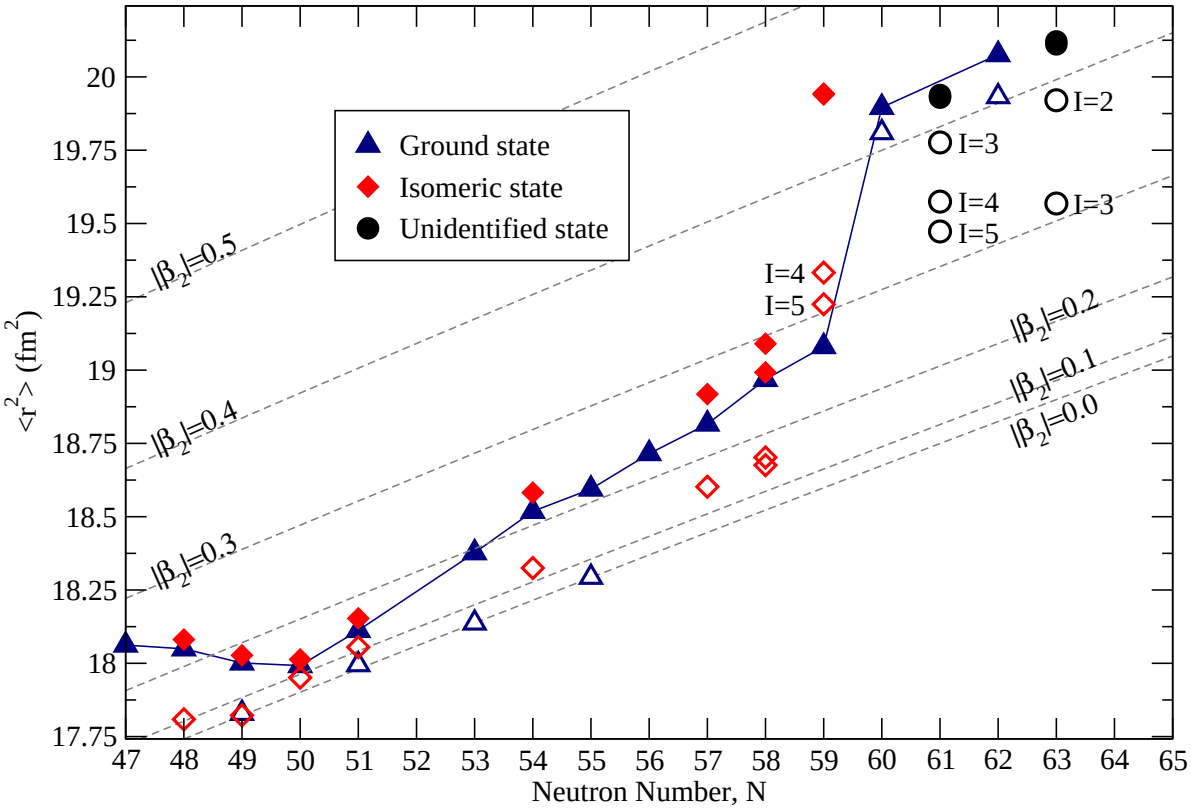

Figure 2. The yttrium mean–square charge radii for the ground and isomeric states. Experimentally determined mean–square charge radii are indicated by filled symbols. Open symbols indicate mean–square charge radii calculated from (1) using only the contribution from the static deformation. Isodeformation contours are included as dashed lines.

Unfortunately, for this ionic ground state transition there is a maximum of only

three hyperfine structure components, which made it impossible to simultaneously determine μ, Q_s, $\delta\langle r^2\rangle^{A,A'}$ and the nuclear spin for ^{97m2,98m,100,102}Y. The situation in ^{100}Y is complicated further as the observed hyperfine structure could arise from either the $\tau_{1/2} = 735$ ms ground state with $I = 1$ or 2, or from the $\tau_{1/2} = 0.94$ s isomeric state at 145 keV with $I = 3, 4$ or 5 [20]. The measured spectrum was fitted for the five different spin possibilities, $I = 1$ – 5, giving various spin–dependent values for the nuclear parameters μ, Q_s and $\delta\langle r^2\rangle^{89,100}$. Unfortunately only one value, with nuclear spin $I = 1$, can be rejected because the analysis gives an unphysically large static deformation parameter $\langle\beta_2\rangle > 0.7$ [10]. The predicted $\langle r^2\rangle$, using a static contribution only for spins $I = 3, 4$ and 5, are included in figure 2. Therefore, a definitive spin assignment is required to define the nuclear properties. This work describes how an unambiguous nuclear spin assignment was achieved for the observed state in ^{100}Y.

2. Preparation to experiment and efficiency tests

In the previous experiment [10], the transition from $^1S_0$ to $^1P_1$ in Y^+ was measured. This kind of transition is preferable for laser spectroscopy when the nuclear spin is known because it significantly reduces the number of hyperfine structure components allowing the whole structure to be measured in a short time. However, to complete the nuclear spin investigations another strong transition needs to be measured with an atomic spin $J > 1$ to complement existing data.

During exploratory efficiency tests, a stable $^{89}Y^+$ ion beam of up to 1 picoampere, produced by a discharge source at the IGISOL [21], was brought onto resonance with ~ 1 mW of laser light. Results showed that the best measured photon to ion efficiency for the transition from the low lying metastable state at 1045.083 cm^{-1} was at least two times lower than the efficiency for the transition previously measured from the ground state. Optical pumping [13] was applied to enhance the population of the 1045.083 cm^{-1} state, improving the spectroscopic efficiency. The $^3D_2$ state population was enhanced by illuminating the ion beam in the cooler/buncher [22] with ~ 5 mW of 363.31 nm laser light. This was produced by frequency doubling the output of a Ti:Sapphire laser which was pumped by a pulsed Nd:YAG laser working at 10 kHz. The effect of the optical pumping and the level scheme for the pumping are shown in figure 3. The optical pumping enhanced the efficiency sufficiently to make the transition from the $^3D_2$ state just possible for on–line measurements.

3. The on–line experiment

Radioactive yttrium isotopes from mass A = 96 to A = 100 were produced at the IGISOL, JYFL by proton induced fission of natural uranium at 30 MeV. The reaction products were thermalized and partially neutralized to singly charged ions in fast flowing helium gas, electrostatically extracted and mass separated. A helium gas pressure of 250 mbar was found to give the best production yields of the radioactive isotopes.

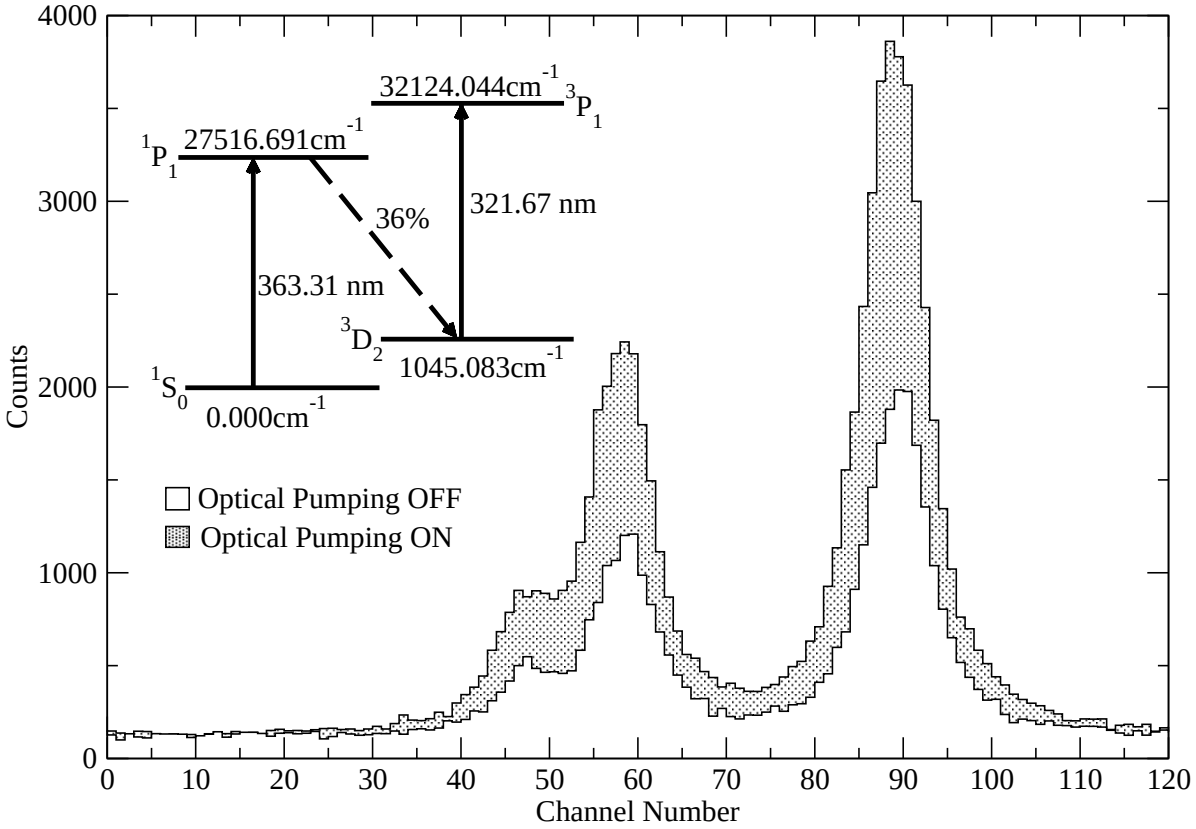

Figure 3. Spectra showing the three hyperfine components for the 321.67 nm transition in $^{89}Y^{+}$ with and without optical pumping. Insert shows the pumping scheme used.

In order to keep the plasma in the reaction part of the chamber, and slow down the fast fission fragments, a thin separation foil made from ^{89}Y was used [21]. Ion rates ranged from 2,100 ions/s for A = 100 to 2,800 ions/s for A = 98, the most strongly produced. The $^{89}Y^{+}$ beam produced from recoils from the thin ^{89}Y foil had an ion rate of 86,000 ions/s.

A dye mixture of Rhodamine 6G and Rhodamine 640 in a Spectra Physics 380 dye laser with an intra cavity β–BBO frequency doubling crystal were used to generate 0.8 mW of 321.67 nm UV light. The laser was locked to the iodine absorption line at 15526.1851 cm^{-1} [23]. For the optical pumping step less than 5 mW of laser power was produced at 363.31 nm wavelength. Spectra were taken for stable ^{89}Y and radioactive isotopes ^{96,98,99}Y to provide calibration of the mass and field factors of the isotope shift [24] and the hyperfine A and B coefficients for the 321.67 nm transition.

The spectra of the yttrium isotopes measured using optical pumping are presented in figure 4. Complete structures were measured for ^{89,96,98,99}Y. Due to low yield and the distribution of spectral strength over many hyperfine structure components, it was necessary, but sufficient, to select only the two strongest components of the ^{100}Y structure. The mass and field factors for the 321.67 nm transition, along with the hyperfine A and B coefficients measured for ^{89}Y and ^{99}Y in this work, were used together

with the data from [10] to estimate the location of these strongest hyperfine components of ^{100}Y for possible spin values in the range $I = 1$ to 5.

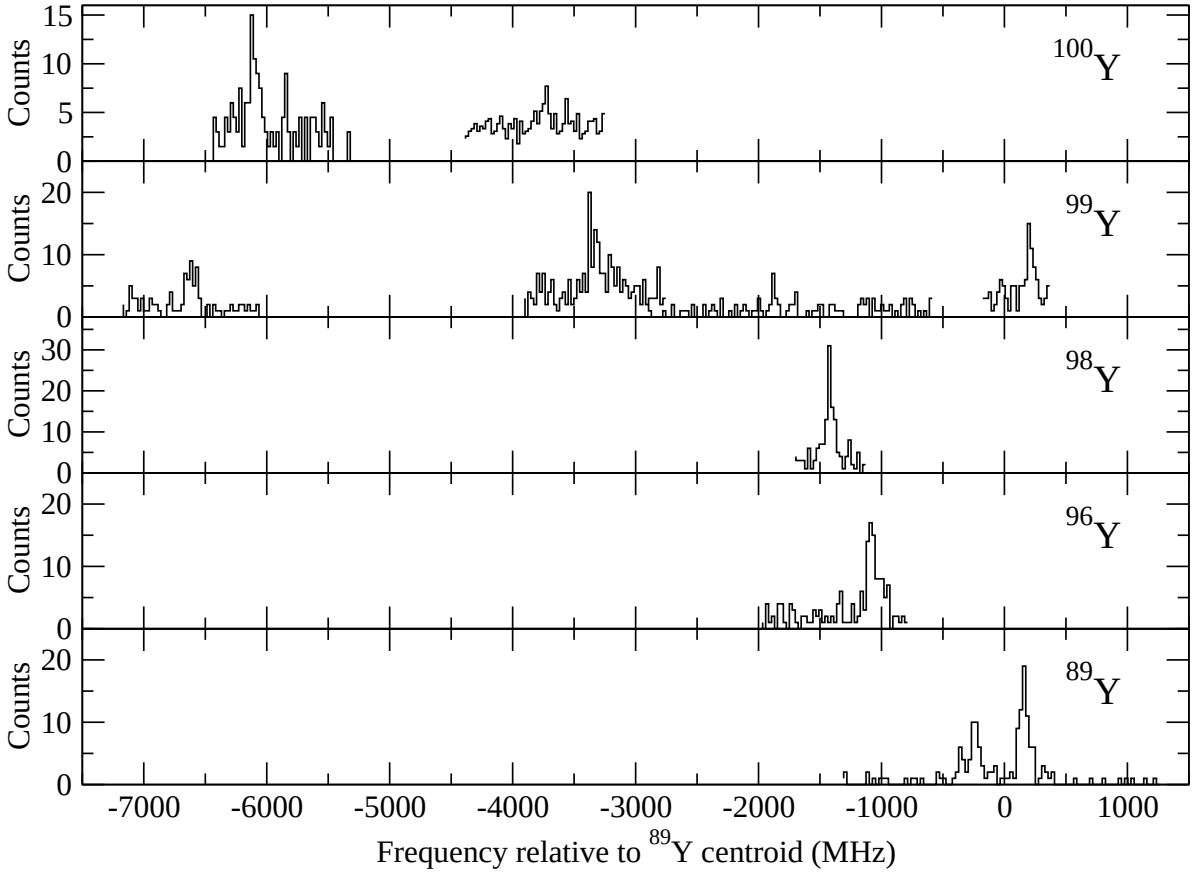

Figure 4. Resonance fluorescence spectra for ^{89,96,98,99}Y and two peaks from ^{100}Y for the ionic transition at 321.67 nm using optical pumping.

4. Data analysis

The hyperfine splitting of an atomic or ionic energy level is given by [19]:

$$E_{\rm hfs} = \frac{A}{2}K + \frac{B}{4}\frac{\frac{3}{2}K(K+1) - 2I(I+1)J(J+1)}{I(2I-1)J(2J-1)}. \tag{5}$$

where K=$F(F$+1)$-J(J$+1)$-I(I$+1), F is the total angular momentum (where $\mathbf{F}$=$\mathbf{I}$+$\mathbf{J}$) and A and B are the magnetic dipole and electric quadrupole hyperfine structure coefficients, respectively. These parameters are related to the nuclear magnetic dipole moment, μ, and spectroscopic quadrupole moment, Q_s, via:

$$A = \frac{\mu \mathrm{B_{el}}}{IJ}, \qquad B = eQ_s \left\langle \frac{\partial^2 V_{\rm el}}{\partial z^2} \right\rangle. \tag{6}$$

As the magnetic field, $\mathrm{B_{el}}$, and the gradient of the electric field, $\langle \partial^2 V_{\rm el}/\partial z^2 \rangle$, produced by the atomic electrons at the nucleus are independent of the isotope, the magnetic

Table 1. Isotope shifts, $\delta\nu^{89,A}$, relative to ^{89}Y, and the hyperfine A and B parameters for the lower and upper states extracted from the analysis of the on–line data. Quoted errors are the statistical error arising from uncertainties in the fitting of the spectra.

Mass A	I^π	$\delta\nu^{89,A}$ (MHz)	$A(^3D_2)$ (MHz)	$A(^3P_1)$ (MHz)	$B(^3D_2)$ (MHz)	$B(^3P_1)$ (MHz)
89	$\frac{1}{2}^-$	0	−220.17(23)	−97.98(39)	–	–
96	0^-	−1068(10)	–	–	–	–
98	0^-	−1414(4)	–	–	–	–
99	$\frac{5}{2}^+$	−2550(10)	+1023(4)	+455(2)	+200(38)	−145(10)

moment, μ^x, and the spectroscopic quadrupole moment, Q_s^x, for an isotope x can be determined from:

$$A^x = \frac{\mu^x}{I^x}\frac{I^y}{\mu^y}A^y\ , \qquad B^x = \frac{Q_s^x}{Q_s^y}B^y \tag{7}$$

where the hyperfine parameters A^y and B^y, moments μ^y and Q_s^y, and the nuclear spin, I^y, are known for a reference isotope y.

The change in mean–square charge radius between two isotopes, $\delta\langle r^2\rangle^{A,A'}$, is related to the measured isotope shift, $\delta\nu^{A,A'}$, via [24]:

$$\delta\nu^{A,A'} = M\frac{A' - A}{AA'} + F\delta\langle r^2\rangle^{A,A'} \tag{8}$$

where M and F are the transition dependent, but isotope independent, mass and field factors respectively.

The nuclear spin determination is based on the predictions of the hyperfine structure constants and isotope shifts for the possible spin values. As the hyperfine structure is dominated by the magnetic dipole interaction, it was essential to find very accurately the ratio of hyperfine A values for the upper and lower states involved in the transition. Spectra of ^{89}Y measured during the off–line tests were fitted using a chi–squared minimization technique to extract the centroid of the structure and the hyperfine A parameters for the lower $^3D_2$ and upper $^3P_1$ states. A weighted average over all the individual measurements gave the final values of $A(^3D_2)$=−220.17(23) MHz and $A(^3P_1)$=−97.98(39) MHz, with their ratio $A(^3P_1)/A(^3D_2)$=+0.445(2). From the data in table 1, it can also be seen that the hyperfine A factors for ^{99}Y have the same ratio, +0.445(3), which indicates that there is no significant hyperfine anomaly in this transition.

Spectra for ^{96,98,99}Y measured during the on–line experiment were also fitted using a chi–squared minimization routine to obtain the centroids and the hyperfine structure parameters. To eliminate any time dependent frequency drifts, the reference isotope ^{89}Y was regularly measured between measurements of radioactive isotopes. Table 1 displays the isotope shifts relative to the reference ^{89}Y determined from the fitted centroids and the hyperfine structure parameters A and B.

5. Spin determination of ^{100m}Y

The isotope shifts given in table 1 were combined with those measured previously in the 363.31 nm transition [10] via a King Plot [24], as shown in figure 5. Using the field, $F_{363} = -3181(57)$ MHz fm^{-2}, and mass, $M_{363} = +1789(40)$ GHz, factors determined for the 363.21 nm ground state transition [10], the King Plot allowed the field and mass factors of the 321.67 nm transition measured in this work to be evaluated as $F_{321} = -1343(25)$ MHz fm^{-2} and $M_{321} = +107(17)$ GHz respectively.

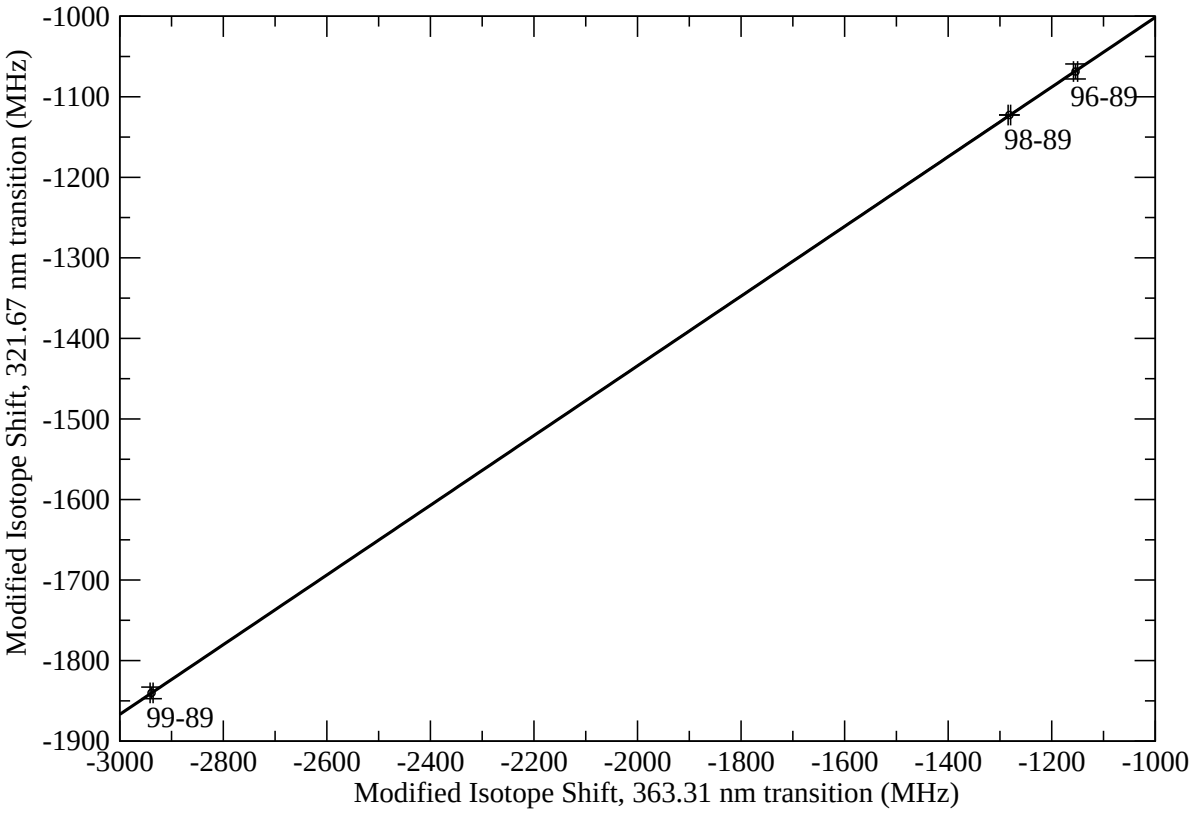

Figure 5. King Plot of the modified isotope shifts of the ^{96,98,99}Y isotopes relative to the reference isotope ^{89}Y obtained from the 321.67 nm transition plotted against the modified $\delta\nu^{89,96}$, $\delta\nu^{89,98}$ and $\delta\nu^{89,99}$ from the 363.31 nm transition.

The isotope shifts and nuclear moments evaluated in reference [10] for spin values $I = 1$ to 5 were used with the calibration data obtained in this work to predict the hyperfine structure and centroid of the produced ^{100}Y state relative to the centroid of the ^{89}Y structure for the $^3D_2$ to $^3P_1$ transition for each possible spin. The $\delta\langle r^2\rangle$, μ and Q_s values from reference [10], along with the predicted isotope shifts relative to the ^{89}Y centroid and hyperfine structure coefficients for the $^3D_2$ level are given in table 2 for each possible spin considered. The hyperfine parameters for the $^3P_1$ level were estimated using the values calculated for the $^3D_2$ level, the ratio of A factors determined from ^{89}Y and the ratio of B coefficients from ^{99}Y.

Figure 6 illustrates the predicted spectra for the nuclear spins $I = 1$ to 5 together

Table 2. The spin–dependent values of $\delta\langle r^2\rangle^{89,100}$ and nuclear moments from reference [10] along with the predicted isotope shift and hyperfine structure constants for all possible spin assignments.

Spin I	$\delta\langle r^2\rangle^{89,100}$ (fm^2)	$\delta\nu^{89,100}$ (MHz)	μ (μ_N)	$A(^3D_2)$ (MHz)	Q_s (b)	$B(^3D_2)$ (MHz)
1	1.978	−2624(4)	1.31(1)	+1049(8)	0.82(9)	+106(26)
2	1.955	−2593(4)	2.18(1)	+873(4)	1.45(16)	+187(46)
3	1.946	−2579(4)	2.55(1)	+681(3)	1.71(19)	+221(54)
4	1.940	−2572(4)	2.75(1)	+551(2)	1.85(20)	+239(59)
5	1.937	−2567(4)	2.88(2)	+461(2)	1.95(21)	+252(62)

with the two experimentally measured peaks for ^{100}Y. It can be seen that the two measured peaks are only matched with the predicted spectrum for the nuclear spin $I = 4$. The structure observed in this work, and in the work of reference [10], therefore arises from the $\tau_{1/2} = 0.94$ s isomeric state in ^{100}Y (which is either spin 3, 4 or 5 [20]) rather than from the lower spin ground state.

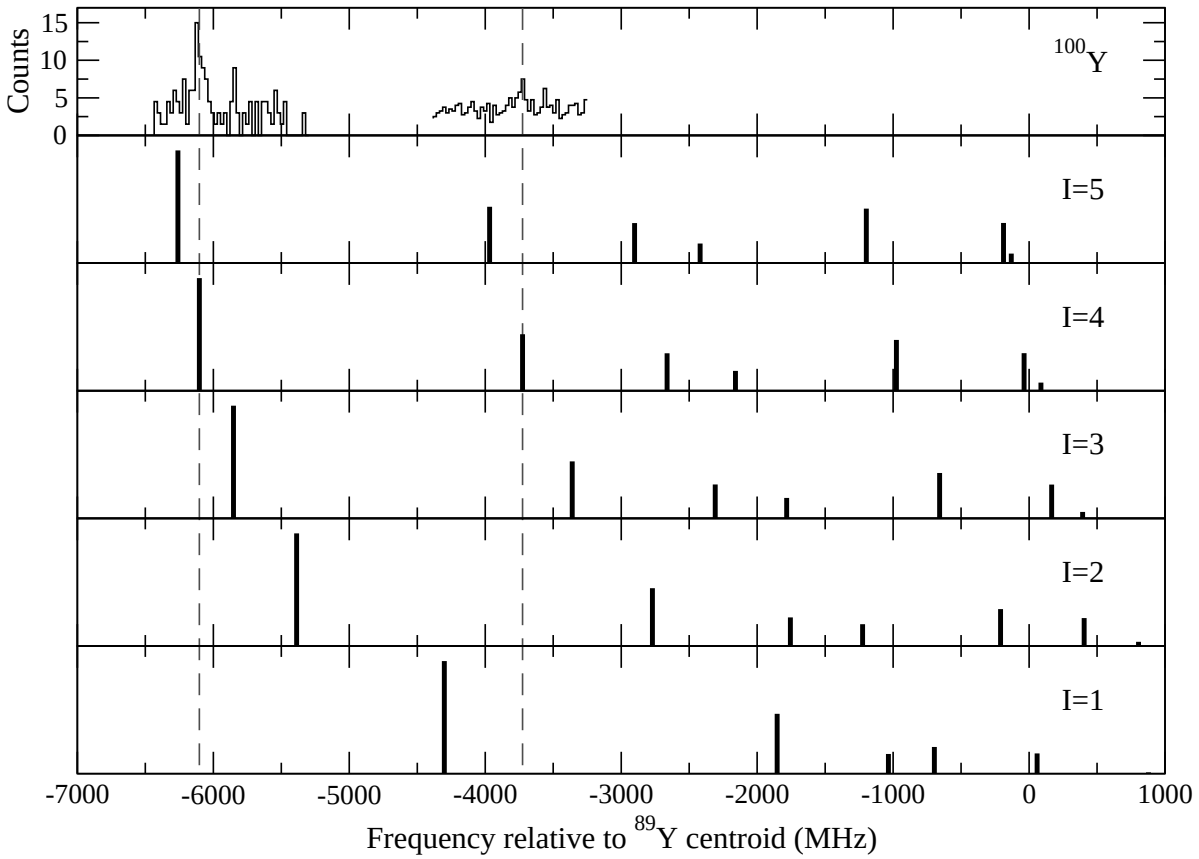

Figure 6. The predicted spectra of ^{100}Y for the nuclear spin I=1,2,3,4,5 with two measured peaks from ^{100}Y.

The uncertainty in the predicted centroid positions is only $\sim 0.2\%$, which is too

small to significantly affect the predicted peak positions. The magnetic dipole and electric quadrupole moments are known with a precision of 1% and 11% respectively. These give, together with the statistical errors from the fitting routine, a precision of the A and B values of 1% and 25% respectively. As the hyperfine structure is dominated by the magnetic dipole interaction, the 25% uncertainty on the B coefficient has a negligible effect on the predicted spectra.

6. Discussion and Interpretation

The unambiguous spin assignment of ^{100m}Y allows the nuclear deformation to be determined from the data of reference [10], where the full hyperfine spectrum was measured. As presented in figure 2, ^{100m}Y follows the sudden shape change at $N = 60$ observed in neighbouring isotopes. For spin $I = 4$, $\langle\beta_2\rangle = +0.35(4)$ was taken from the data of reference [10] and it shows that the nucleus has a prolate shape. The difference between the deformation obtained from the isotope shift data and that obtained from the hyperfine structure data, as seen in figure 2, is quite large which indicates a sizable dynamic contribution to the deformation.

The behaviour of ^{100m}Y reported here is notably different to that observed in the ground states of its neighbouring even–N isotopes, ^{99,101}Y, which display static and rigid deformations. The nature of the deformation in ^{100m}Y does however closely resemble that observed in the deformed isomeric state of ^{98}Y [10]. In reference [10] it was possible to show, irrespective of the spin assignment in ^{98m}Y, that this system had a large mean–square charge radius and yet a relatively small (but prolate) quadrupole deformation. The $N = 59$ isomer was reported to be the softest configuration in yttrium observed to date and it was believed that after the shape change, more rigidly deformed shapes were being observed with increasing neutron number. For the odd–N isomeric system ^{100m}Y this is clearly not the case. Moreover if the ^{102}Y structure reported in reference [10] arises from the isomeric configuration then this nucleus must also be assigned a soft structure (although a spin determination will be required before a definitive assignment can be made). Unlike the zirconium isotopes beyond $N = 59$, the known yttrium systems now show an alternating character in their deformation between rigid shapes observed in the even–N ground states to the soft deformations displayed by the odd–N isomers.

The assignment of $I = 4$ for ^{100m}Y also gives information on the probable two–quasiparticle configuration of this isomer. Studies of the β^-–decay from this state, and the lowest–lying single–particle Nilsson orbitals in neighbouring nuclei, led Lhersonneau *et al* to conclude that the most likely two–quasiparticle configurations were either $\{\pi[422]5/2 \otimes \nu[411]3/2\}\, 4^+$ or $\{\pi[422]5/2 \otimes \nu[532]5/2\}\, 5^-$ [25]. Also, the configuration $\{\pi[303]5/2 \otimes \nu[411]3/2\}\, 4^-$ must be considered, as this corresponds to the parallel–coupled partner of the $\{\pi[303]5/2 \otimes \nu[411]3/2\}\, 1^-$ configuration tentatively assigned to the ground state of ^{100}Y [26]. Of these candidates, only the $K^\pi = 5^-$ possibility is eliminated by the spin assignment of $I = 4$.

The two remaining possible configurations can be distinguished by considering the

magnetic moment. The moment for a two–quasiparticle state can be estimated using the additivity theorem [27]:

$$\mu = \frac{I}{I+1}\left(g_R + g_{K_\pi}K_\pi + g_{K_\nu}K_\nu\right) \tag{9}$$

where K_π and K_ν are the projections of the uncoupled proton and neutron spins along the nuclear symmetry axis respectively, and $I = |K_\pi \pm K_\nu|$. The g–factors $g_{K_\nu} = -0.48(3)$ and $g_{R_\nu} = +0.26(4)$ for the $\nu[411]3/2$ orbital were deduced from laser spectroscopic [11, 12] and integrated perturbed angular correlation [28], measurements of ^{101}Zr, while $g_{K_\pi} = +1.61(4)$ and $g_{R_\pi} = 0.44(10)$ can be extracted for the $\pi[422]5/2$ Nilsson state using the magnetic moment, $\mu = +3.18(2)\ \mu_N$, intrinsic quadrupole moment, $Q_0 = +4.34(48)$ b [10] and $(g_K - g_R)/Q_0 = 0.27(3)$ [26] measured for ^{99}Y. The g–factors for the $\pi[303]5/2$ state can be estimated as $g_{K_\pi} \simeq g_{R_\pi} = Z/A = 0.39$ because $(g_K - g_R)/Q_0 \sim 0$ for this orbital [26]. Using equation 9, these g–factors give estimates of $\mu = +2.92\ \mu_N$ and $\mu = +0.46\ \mu_N$ for the $K^\pi = 4^+$ and $K^\pi = 4^-$ configurations respectively. Clearly, only the $\{\pi[422]5/2 \otimes \nu[411]3/2\}\, 4^+$ two–quasiparticle configuration gives a moment that is consistent with the measured value of $+2.75(1)\ \mu_N$.

7. Conclusion

In order to extend the investigation of the nuclear shape and deformation of the yttrium isotope chain above the sudden shape change at $N = 60$, the nuclear spin of ^{100m}Y has been measured by collinear laser spectroscopy with optical pumping at the IGISOL facility at the University of Jyväskylä, Finland.

The unambiguous spin assignment $I = 4$ provides critical information about the magnetic dipole and electric quadrupole moments, mean–square charge radii difference, $\delta\langle r^2\rangle^{89,100m}$, the nuclear deformation and the two–quasiparticle configuration. It is observed that ^{100m}Y follows the sudden shape change to a strongly prolate shape, seen in the neighbouring isotope chains: Sr, Rb, Zr and Nb. However, unlike the ^{99,101}Y isotopes, this state in ^{100}Y also has a strong dynamic component to its deformation. This discrepancy illustrates the richness of nuclear behaviour in this region, and provides compelling reasons for extending the nuclear spin investigations for the remaining ^{100g,102g,m}Y isotopes.

Acknowledgments

This work has been supported by the UK STFC, the EU 6th Framework programme "Integrating Infrastructure Initiative–Transnational Access", Contract No. 506065 (EURONS) and by the Academy of Finland Centre of Excellence Programme 2006–2011 (Nuclear and Accelerator Based Physics Programme at JYFL).

References

[1] Hager U *et al* 2006 *Phys. Rev. Lett.* **96** 042504
[2] Hager U *et al* 2007 *Nucl. Phys.* A **793** 20
[3] Wu C Y *et al* 2004 *Phys. Rev.* C **70** 064312
[4] Urban W *et al* 2001 *Nucl. Phys.* A **689** 605
[5] Keim M *et al* 1995 *Nucl. Phys.* A **586** 219
[6] Thibault C *et al* 1981 *Phys. Rev.* C **23** 2720
[7] Anselment M *et al* 1987 *Z. Phys.* A **326** 493
[8] Buchinger F *et al* 1990 *Phys. Rev.* C **41** 2883
[9] Lievens P *et al* 1992 *Phys. Rev.* C **46** 797
[10] Cheal B *et al* 2007 *Phys. Lett.* B **645** 133
[11] Thayer H *et al* 2003 *J. Phys. G: Nucl. Part. Phys.* **29** 2247
[12] Campbell P *et al* 2002 *Phys. Rev. Lett.* **89** 082501
[13] Cheal B *et al* 2009 *Phys. Rev. Lett.* **102** 222501
[14] Charlwood F C *et al* 2009 *Phys. Lett.* B **674** 23
[15] Federman P and Pittel S 1979 *Phys. Rev.* C **20** 820
[16] Werner T R *et al* 1994 *Nucl. Phys.* A **578** 1
[17] Verma S, Dar P A and Devi R 2008 *Phys. Rev.* C **77** 024308
[18] Myers W D and Schmidt K H 1983 *Nucl. Phys.* A **410** 61
[19] Kopfermann H 1958 *Nuclear Moments* (New York: Academic)
[20] Singh B 2008 *Nucl. Data Sheets* **109** 297
[21] Äystö J 2001 *Nucl. Phys.* A **693** 477
[22] Nieminen A *et al* 2002 *Phys. Rev. Lett.* **88** 094801
[23] Gerstenkorn S and Luc P 1980 *Atlas du Spectre D'Absorption de la Molecule d'Iode* (Orsay, France: Laboratoire Aime-Cotton)
[24] King W H 1984 *Isotope Shifts in Atomic Spectra.* (New York: Plenum)
[25] Lhersonneau G *et al* 2002 *Phys. Rev.* C **65** 024318
[26] Wohn F K *et al* 1983 *Phys. Rev. Lett.* **51** 873
[27] Hooke W M 1959 *Phys. Rev.* **115** 453
[28] Orlandi R *et al* 2006 *Phys. Rev.* C **73** 054310